Hazardous trace particles in the airborne thoracic fraction: Temporal variation, source analysis, and health risk assessment in a megacity

Omar Ramírez[a,b*], A.M. Sánchez de la Campa[b,c], Daniel Sánchez-Rodas[b,d], Jesús D. de la Rosa[b,c]

[a] Department of Civil and Environmental, Universidad de la Costa, Calle 58 #55-66, 080002 Barranquilla, Colombia.
[b] Associate Unit CSIC-University of Huelva "Atmospheric Pollution", Centre of Research in Sustainable Chemistry-CIQSO, Campus de El Carmen, 21071, Huelva, Spain.
[c] Department of Earth Sciences, University of Huelva, Campus de El Carmen, 21071, Huelva, Spain.
[d] Department of Chemistry and Materials Science, University of Huelva, Campus de El Carmen, 21071, Huelva, Spain.

[*] Corresponding author. E-mail: oramirez@cuc.edu.co, omar.ramirez@unad.edu.co (Ramírez, O.).

Abstract

Deleterious health effects of thoracic fraction seem to be more related to the chemical composition of particles, than to their mass concentration. The presence of hazardous materials in PM_{10}, such as heavy metals and metalloids, implies risks for human health. This study analyzed eleven trace elements (Cd, Cr, Pb, Zn, Cu, Ni, Sn, Ba, Co, As, and Sb) in 315 samples of ambient PM_{10} collected at an urban background site in a Latin American megacity (Bogota) for one year. The concentration and temporal variability of these elements was examined, finding that Cu (52 ng/m^3), Zn (44 ng/m^3), Pb (25 ng/m^3), and Ba (20 ng/m^3) were the traces with the highest concentrations, particularly during a dry season (January to March) characterized by BBQ charcoal combustion and forest fires. Differences between weekdays and weekends were also identified. Enrichment factor analysis indicated that Zn, Pb, Sn, Cu, Cd, and Sb mainly originated from anthropogenic sources. Speciation analysis of inorganic Sb was conducted, detecting that Sb(V) was the main Sb species present in the PM_{10} samples (> 80%). Six factors were identified by PMF model: fuel combustion and crustal dust (54%), road dust (21%), traffic-related emissions (8%), copper smelting (8%), iron and steel industry (5%), and an unidentified industrial sector (4%). A health risk assessment was performed for carcinogenic elements, finding that the cancer risk for inhalation exposure to Co, Ni, As, Cd, Sb(III), and Pb was negligible for both children and adults at the sampling site. For adults, adjusted Cr(VI) was slightly higher than the minimum acceptable risk level considering the entire study period (1.4 x 10^{-6}). The average risk values for both adults and children decreased in the following order: adjusted Cr(VI) > Co > As > Sb(III) > Cd > Ni > Pb.

Keywords

Heavy metals; PM_{10}; PMF model; Cancer risk; Antimony speciation; Source apportionment.

1. Introduction

Airborne particulate matter (PM) is a complex mixture of aerosols with different sizes and a diverse chemical composition. The thoracic fraction, with an aerodynamic diameter < 10 μm (PM_{10}), has been related to global morbidity and mortality levels (WHO, 2016; IHME, 2017). This pollutant is identified as one of the major urban air pollutants, particularly in Latin American cities where urban pollution levels are high (Green and Sanchez, 2013, UNEP, 2016).

Health impacts of thoracic fraction seem to be more related to the chemical composition of particles (i.e., toxic elements), than to their mass concentration (Franklin et al., 2008, Jin et al., 2019). Therefore, the existence of hazardous materials in PM, such as heavy metals and metalloids, implies risks for human health, although their contribution to the total mass is not significant. Several studies have associated exposure to heavy metals and metalloids particles (HMMP) with cases of asthma, allergies, lung injuries, neuronal damage, cardiovascular disease, impaired blood pressure, deterioration of renal function, and low birth weight (Franklin et al., 2008; WHO, 2008; Bell et al., 2010; Jaishankar et al., 2014; Gehring et al., 2015; Lelieveld et al., 2019). PM in outdoor air pollution has been classified as a group 1 carcinogenic agent by the International Agency for Research on Cancer as a consequence of the presence of toxic compounds (IARC, 2016). A thorough understanding of the temporal variability and sources of HMMP is critical to assess their impacts on human health and the environment.

The main anthropogenic sources of HMMP have been associated to coal and oil combustion, metallurgy/ceramic/cement industry, waste incineration, and traffic-related emissions (Khillare and Sarkar, 2012; Duan and Tan, 2013; Tan et al., 2014; Hsu et al., 2016; Cheng et al., 2018). These activities are mainly concentrated in densely populated cities, where citizens are constantly exposed to airborne metal particles. One such case is Bogota (the capital of Colombia), a Latin American megacity of over 8 million inhabitants (DANE, 2010) and one of the most densely populated tropical cities in the world (18,300 hab/km^2; Demographia, 2019), which is exposed to poor air quality (Molina et al., 2004; Zhu et al., 2012; IDEAM, 2016; UNEP, 2016). PM_{10} is the most significant pollutant affecting Bogota's air quality (SDA, 2018, 2017) and citizens' health, especially children aged < 5 years-old (Hernández et al., 2013). This situation has been identified as a matter of great relevance by citizens (Ramírez et al., 2017). Despite this, there is a lack of research into the temporal variability, origin, and health implications of airborne hazardous materials as HMMP.

Previous studies have analyzed the concentration of trace elements (such as Pb, Cr, Cu, Zn, Ni, Cd, Mn, among others) in samples of PM_{10} collected during short periods of time (< 3 months) at residential and industrial areas in Bogota (Pachón and Sarmiento, 2008; SDA, 2009; Vargas et al., 2012). However,

there are no studies analyzing the temporal variability of HMMP during a continuous year of PM_{10} sampling, their main sources, and the human health risk due to the exposure to potentially toxic airborne elements. Although speciation studies of emerging pollutants in the atmosphere, such as Sb, are scarce (He et al., 2019), an inorganic Sb speciation analysis of PM_{10} samples was conducted in the present study. This metalloid is a representative redox-sensitive trace element in environment, its toxicity is related to the oxidation state (Wu and Sun, 2016), and the most frequently oxidation states are III and V, being Sb(III) more toxic than Sb(V) (Filella et al., 2002). Thus, the aim of this study is to expand the current knowledge of selected heavy metals (Cd, Cr, Pb, Zn, Cu, Ni, Sn, Ba, and Co) and metalloids (As and Sb) in the thoracic fraction at an urban background site in one of the main Latin American megacities.

2. Materials and methods

2.1. Study area and PM_{10} sampling

Characteristics of the study area and the sampling conditions, including meteorological parameters, have been described in previous studies (Ramírez et al., 2018a, 2018b). Briefly, Bogota has a vehicle fleet dominated by private vehicles (> 2.2 millions) and motorcycles (467,000), of which 95% use gasoline. There are also buses, dump, and heavy-duty trucks which use diesel (SDM, 2017). Bogota has nearly 2,000 industrial smokestacks (including chemical, paper, cement, plastic, beverage and food industry, metallurgy, paint manufacturing, among others) which emit PM as a result of productive processes (SDA, 2009). The sampling site was located at the Universidad Libre campus (Fig. SD1 on Supplementary Data), which is considered an urban background site. The meteorological data were obtained from the CAR air quality station, located at ~ 1.5 km from the sampling point. Daily PM_{10} samples were collected (24±1h) between 01 June (2015) and 31 May (2016), obtaining 315 filters in total. An intense dry season was recorded during the study period between December (2015) and February (2016), which induced local and regional forest fires (Ramírez et al., 2018b).

2.2. Chemical characterization

Following a modified method proposed by Querol et al. (2008), 75 cm^2 of each filter were acid digested (HNO_3, HF, $HClO_4$), and the residue recovered with 5% HNO_3 in a Milli-Q H_2O solution. Selected trace metals and metalloids (Cd, Cr, Pb, Zn, Cu, Ni, Sn, Ba, Co, As, and Sb) were analyzed by ICP-MS. The quality of the results was controlled by certified reference standards (NBS1633b) and by adding Rh at a known concentration as internal standard. The average precision and the accuracy were within normal analytical errors (5-10%) and detection limit for most elements in solution was 0.01 ppb.

2.3. Identification of sources

2.3.1. Enrichment factor (EF)

EF has been widely used to determine the geogenic and anthropogenic origin of chemical elements. EF was calculated for eleven selected metals and metalloids, using Equation 1 (Zoller et al., 1974).

$$EF_{[X]} = \frac{[X]_{sample}/[Rf]_{sample}}{[X]_{crust}/[Rf]_{crust}} \qquad [1]$$

where [*X*] is the concentration of HMMP under consideration and [*Rf*] is the concentration of the reference element. Enrichment factors were calculated based on the upper continental crust composition (Rudnick and Gao, 2003). The reference metals commonly used in similar studies were Al, Fe, and Mn (Tan et al., 2014; Zhou et al., 2014; Pasha and Alharbi, 2015). This study selected Al considering its abundance on the upper continental crust (Rudnick and Gao, 2003). EF values > 10 typically indicate enrichment of the sample by anthropogenic activities, meaning 10 < EF < 100 a moderate enrichment, and EF values > 100 a great enrichment. EF < 10 suggests a predominantly natural origin where values close to unity indicate a crustal origin (Zhou et al., 2014; Jena and Singh, 2017).

2.3.2. Antimony speciation analysis

Circular portions of 1.2 cm^2 of selected PM_{10} filters were extracted for Sb speciation, obtaining concentration of Sb(III) and Sb(V), following a procedure described by Sánchez-Rodas et al. (2017). The analytical procedure consisted of a liquid extraction with a $NH_2OH{\cdot}HCl$ solution aided with microwave radiation. The Sb speciation analysis of the liquid extract was achieved combining high performance liquid chromatography, hydride generation and atomic fluorescence spectroscopy (HPLC-HG-AFS). Antimony speciation was performed for PM_{10} samples with significant Sb concentrations (> 4 ng/m^3) and a percentage of Sb extraction above 50%.

2.3.3. Source apportionment

The Positive Matrix Factorization (PMF) model was developed by Paatero and Tapper (1994) and Paatero (1997). EPA-PMF 5.0 was the reference model used. The mathematical algorithms, as well as the conceptual explanation of the model, are presented in US EPA (2014). Factor contributions and profiles are derived by the PMF model minimizing the objective function *Q* (Equation 2).

$$Q = \sum_{i=1}^{n}\sum_{j=1}^{m}\left[\frac{x_{ij} - \sum_{k=1}^{p} g_{ik} f_{kj}}{u_{ij}}\right]^2 \qquad [2]$$

where n is the number of samples, m depicts the number of species, p is the number of sources included in the analysis, x_{ij} is the concentration of i sample and j chemical species, g_{ik} represents the contribution of k factor to i sample, f_{kj} is j species fraction from k source, and u_{ij} is the uncertainty of j species in i sample (US EPA, 2014). Concentrations and uncertainties of each chemical species were the input data. The uncertainties were mainly associated with analytical procedures errors. This study used destructive analysis of the filters where PM was collected, therefore blank subtraction uncertainties have been incorporated following the method proposed by Amato et al. (2009). 10% extra uncertainty was added to consider analytical and measurement errors not included in previous calculations. Elements were classified using the signal-to-noise ratio (S/N > 2.0 = strong, 2.0 > S/N > 0.2 = weak, and S/N < 0.2 = bad variables). The percentage of data above detection limit was used as a complementary criterion. In the current study, Ba, Cr, Zn, and Ni were set as "weak" and Cu, Co, Cd, As, Sn, Sb, and Pb as "strong". The optimal number of factors was obtained by analyzing the scaled residuals, the G-space plots, the physical meaningfulness of the factor profiles, and the proximity of Q_{robust} and Q_{theory} (JRC, 2019), being $Q_{theory} = nm - p(n+m)$ (US EPA, 2014).

2.4. Health risk assessment

In this study, the carcinogenic health risks were calculated via the inhalation exposure to HMMP in PM_{10} according to Environmental Protection Agency method (US EPA, 2011). Arsenic, Ni, Cd, Cr(VI), Co, Sb(III), and Pb are categorized as follows: As, Ni, Cd, and Cr(VI) are *carcinogenic to humans* (group 1; IARC, 2012), Co and Sb(III) are *possibly carcinogenic to humans* (group 2B; IARC, 1989, 2006a), and inorganic Pb is *probably carcinogenic to humans* (group 2A; IARC, 2006b). This research measured the total concentration of Cr, including Cr (III) and Cr(VI). The first is classified as Group 3 (*not classifiable for human carcinogenicity*) and the second as Group 1 (*carcinogenic to humans*) (IARC, 1990, 2012). This study assumed that the Cr(VI) to Cr (III) ratio is 1:6 (Park et al., 2008; Hsu et al., 2016). Accordingly, the concentration of adjusted Cr(VI) was estimated as one seventh of the total Cr concentration.

It was assumed that adults and children living and studying in the study site were potential receptors, and the inhalation was the main pathway of exposure to HMMP in the thoracic fraction as previous studies have reported (Li et al., 2016a; Sah et al., 2019). Exposure concentration (ExpC, $\mu g/m^3$) and risk characterization (RC, dimensionless) for carcinogenic elements were calculated using the Equations 3 and 4, respectively (US EPA, 2011).

$$ExpC = (C * ET * EF * ED *)/AT \qquad [3]$$

$$RC = ExpC * IUR \qquad [4]$$

where C is metal or metalloid concentration in PM_{10} ($\mu g/m^3$), ET represents exposure time (hours/day), EF is exposure frequency (days/year), ED is exposure duration (years), and AT is average lifetime (hours = years x 365 days/year x 24 hours/day). IUR is Inhalation Unit Risk $(\mu g/m^3)^{-1}$ provided by the Integrated Risk Information System - IRIS (https://www.epa.gov/iris), the Office of Environmental Health Hazard Assessment - OEHHA (https://oehha.ca.gov), and the National Research Council (2000). Table 1 shows the values of all the considered parameters. The minimum threshold value for cancer risk is 1×10^{-6}. Below this value risk is negligible, whereas a risk level of 1×10^{-4} (maximum threshold value) or greater is considered serious (US EPA, 2001, 2009).

Table 1. Summary of the parameters considered to evaluate cancer risk.

Parameters	Units	Values		References
		Children	Adults	
ET - exposure time	hours/day	24	24	US EPA, 2001
EF - exposure frequency	days/year	315	315	This study (sampling days)
ED - exposure duration	year	6[a]	24[a]	Wang et al., 2018a US EPA, 2001
AT - average lifetime	hour	74[b]x365x24	74[b]x365x24	The World Bank, 2016
IUR - Inhalation Unit Risk				
Cr(VI)	$(\mu g/m^3)^{-1}$	1.2×10^{-2}		IRIS
Co		7.8×10^{-3}		Dodge and Silva, 2019
Ni		2.4×10^{-4}		IRIS Unit risk of refinery dust was used
As		3.3×10^{-3}		OEHHA Unit risk of inorganic arsenic was used
Cd		1.8×10^{-3}		IRIS
Pb		1.2×10^{-5}		OEHHA Unit risk of inorganic lead was used
Sb(III)		7.1×10^{-4}		National Research Council, 2000 Unit risk of lung cancer was used

[a] Reasonable Maximum Exposure (RME). [b] Life expectancy at birth in Colombia.

3. Results and discussion

3.1. Metals and metalloids levels

The HMMP with the highest concentrations were Cu (52 ng/m^3), Zn (44 ng/m^3), Pb (25 ng/m^3), and Ba (20 ng/m^3) considering the entire study period (Table 2). Other elements such as Cr, Ni, Sb, and Sn obtained values between 1.0 ng/m^3 and 5.0 ng/m^3, while As, Cd, and Co recorded levels < 1.0 ng/m^3. The concentration of HMMP in the thoracic fraction in descending order is as follows: Cu > Zn > Pb >

Ba > Sb > Sn > Cr > Ni > As > Cd > Co.

Table 2. Summary of concentration of selected metals and metalloids in outdoor PM_{10} (ng/m^3).

		As	Ba	Cd	Co	Cr	Cu	Ni	Pb	Sb	Sn	Zn
Whole period	Mean	0.53±0.49	20.4±25.3	0.26±0.25	0.25±0.39	2.92±2.52	51.7±54.1	1.69±1.44	24.8±108	4.74±7.33	3.11±2.70	44.4±45.5
2015	Jun (N=26)	0.22±0.15	13.0±16.6	0.12±0.10	0.40±1.19	2.40±2.66	26.2±15.5	0.56±0.31	3.70±2.61	1.82±1.07	1.76±1.01	26.1±17.8
	Jul (N=28)	0.25±0.15	14.7±11.6	0.15±0.14	0.15±0.15	3.09±2.56	26.9±12.5	0.88±0.55	6.19±8.33	2.40±2.16	2.17±1.68	33.4±21.1
	Aug (N=28)	0.27±0.25	19.7±28.1	0.13±0.15	0.10±0.07	2.45±2.04	42.4±40.1	0.62±0.46	6.72±10.3	2.54±3.20	1.80±1.63	27.5±22.0
	Sep (N=29)	0.38±0.17	16.4±10.6	0.20±0.20	0.19±0.30	4.75±3.55	45.0±18.4	1.33±0.73	4.76±3.98	2.72±2.02	2.14±1.41	48.9±38.5
	Oct (N=28)	0.62±0.54	23.3±14.8	0.28±0.18	0.18±0.10	3.30±2.48	62.2±17.6	0.86±0.45	12.6±13.2	5.82±7.93	3.27±1.73	47.7±32.6
	Nov (N=30)	0.70±0.38	32.4±18.0	0.47±0.42	0.28±0.16	3.67±2.04	54.2±26.2	1.05±0.58	19.5±40.5	7.60±10.8	4.02±2.08	68.2±42.8
	Dec (N=20)	0.40±0.35	38.0±30.0	0.20±0.24	0.17±0.09	2.25±1.46	145±101	0.62±0.44	8.70±12.5	3.07±2.11	2.76±1.68	44.7±24.1
2016	Jan (N=23)	1.20±0.57	43.0±15.7	0.44±0.20	0.51±0.27	4.43±2.30	84.8±122	1.79±0.73	108±210	9.61±9.21	5.86±4.02	108±92.5
	Feb (N=26)	0.76±0.62	12.2±22.3	0.25±0.16	0.35±0.17	2.13±2.89	39.4±18.8	3.55±1.14	16.9±33.0	5.83±9.04	2.83±1.70	31.3±53.1
	Mar (N=28)	0.77±0.75	12.0±52.2	0.38±0.19	0.32±0.17	1.17±1.15	43.9±25.4	4.26±0.64	75.1±278	8.41±13.7	4.30±5.17	20.9±24.6
	Apr (N=24)	0.50±0.27	4.37±8.10	0.31±0.39	0.26±0.12	1.64±1.62	35.6±30.7	3.50±1.14	33.2±102	4.05±2.40	3.59±2.44	30.1±36.9
	May (N=25)	0.31±0.20	20.8±14.5	0.14±0.14	0.16±0.12	3.46±1.83	41.1±9.41	1.25±0.74	10.5±11.1	2.84±1.67	3.08±2.15	52.0±27.2

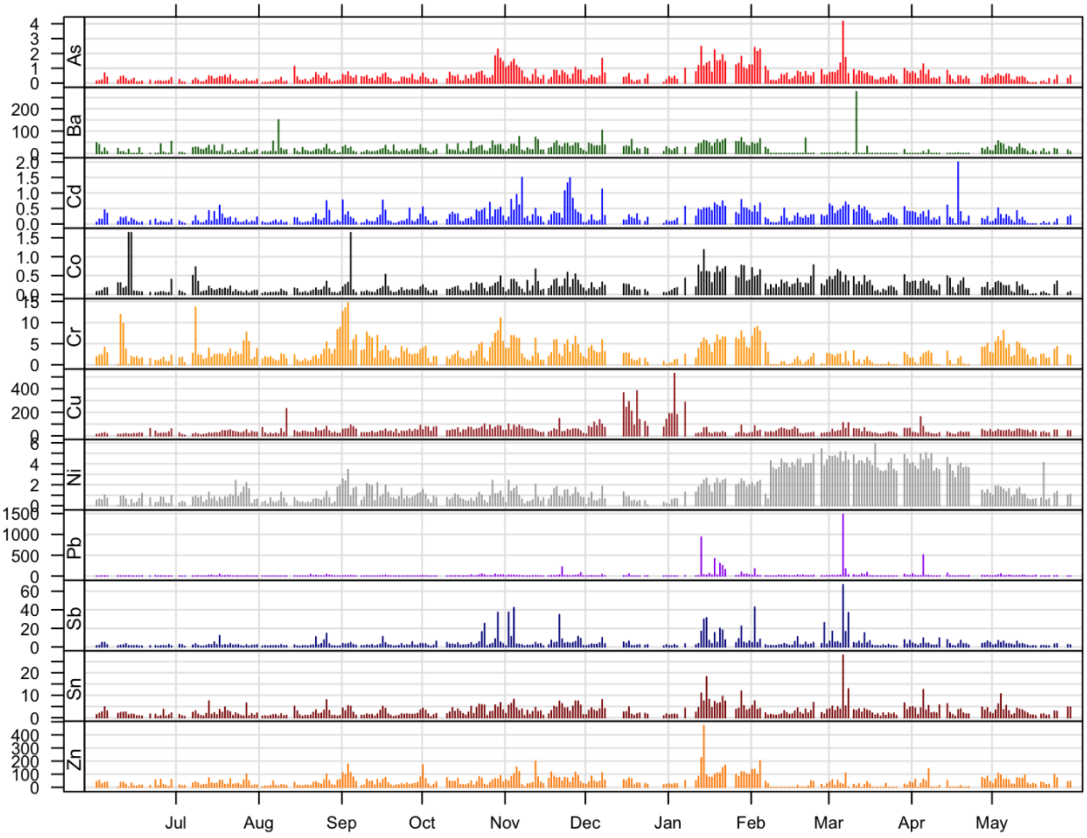

Fig. 1. Temporal variations of the selected metals and metalloids particles.

Daily values of Cu ranged from 5 ng/m^3 to 530 ng/m^3, and Ba, Zn, Pb levels ranged from < 1.0 ng/m^3

to 276 ng/m^3, 471 ng/m^3, and 1,481 ng/m^3, respectively (Fig. 1). Wide concentration ranges indicate a significant dispersion of the dataset, evidenced by high values of standard deviation (Table 2), suggesting the existence of sporadic and seasonal events during the sampling year.

The mean Cu, Pb, and Ba concentrations were significantly higher than those reported at urban background sites in Europeans cities. Copper values exceeded x4 levels found in Budapest (Muránszky et al., 2011) and London (Crilley et al., 2017). Amounts of Pb were threefold and twofold those found in Barcelona (Pérez et al., 2016) and Porto (Albuquerque et al., 2017), respectively. Barium concentrations were two times higher than the levels in Lecce (Cesari et al., 2018) and Tarragona (Moreno et al., 2006). Zinc values showed a different behavior, since the concentrations measured in Bogota were lower than those obtained in most of the aforementioned European cities. Levels of Cu, Pb, Ba, and Zn in Bogota were significantly lower than those measured in Asian cities such as Chengdu (Cheng et al., 2018), Ulsan (Hieu and Lee, 2010), and Delhi (Chandra et al., 2017), which could be explained by the predominance of industrial activities and waste/biomass burning in India and China.

3.2. Temporal variations of selected HMMP

January to March was the season with the highest average concentration of most HMMP with values between 0.51 ± 0.27 ng/m^3 (Co) and 108 ± 210 ng/m^3 (Pb) (Table 2). The largest levels of temperatures and irradiance were recorded during these months, as well as the lowest values of precipitation, due to the influence of the El Niño Southern Oscillation (ENSO) (Ramírez et al., 2018b). These weather conditions contributed to wildfires in rural areas in Bogota (SDA, 2017) and nearby municipalities, and also encouraged barbecues (BBQ) across the city, which is a very common family activity in January. Both wildfires and BBQ charcoal combustion have been identified as important sources of trace metals (Susaya et al., 2010; Kabir et al., 2011; Odigie and Flegal, 2014).

The highest monthly values of Cu were obtained in December-January (85 ng/m^3 - 145 ng/m^3; Table 2). Analyses of the polar plot during these months indicate that the largest concentrations of Cu were obtained from W-SW at wind speeds between 1.2 m/s and 1.6 m/s (Fig. 2A). This highlights the huge influence of anthropogenic sources, such as traffic and industries, located to the west of the study area. The most significant daily concentration of Cu throughout the year was recorded on January 3, 2016 (530 ng/m^3; Fig. 1), the first Sunday of the year, when families usually have BBQ in their homes and authorized public parks in Bogota. Consequently, the massive use of charcoal may be an important urban source of Cu, which agrees with findings from other studies (Susaya et al., 2010; Kabir et al., 2011). Although the impact of charcoal combustion was observed in a specific season, its contribution to trace particles should not be disregarded in other months since several restaurants regularly use charcoal as fuel.

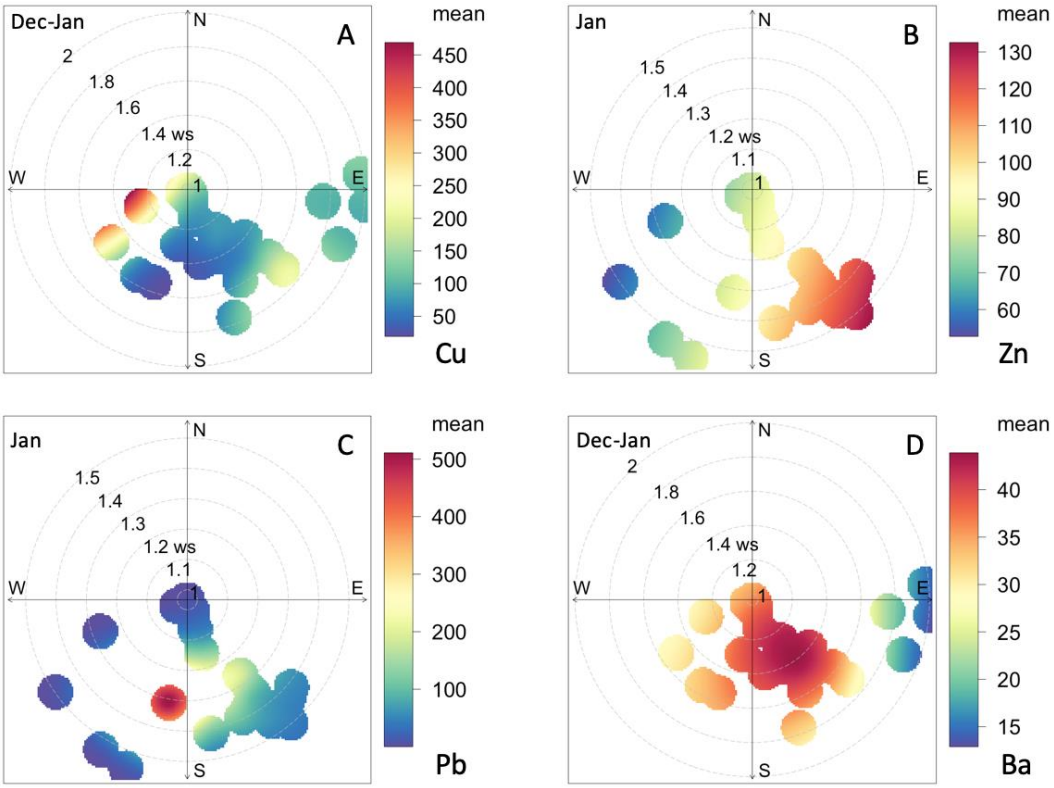

Fig. 2. Polar plots of A) Cu, B) Zn, C) Pb, and D) Ba during months with the highest concentrations.

The largest monthly average value of Zn was found in January (108 ± 92.5 ng/m^3). The highest daily value was measured on January 14, during the first workweek of the year (471 ng/m^3). This could be related to anthropogenic sources, since Zn levels have been typically associated with exhaust and non-exhaust vehicle emissions in urban areas (Councell et al., 2004; Apeagyei et al., 2011). After considering the polar plot for Zn in January (Fig. 2B), it was observed significant contributions of this metal from SE. Bogota's downtown is located at ~ 6 km in that direction (Fig. SD1), which supports the anthropogenic origin of this element.

The maximum monthly Pb concentration was also obtained in January (108 ± 210 ng/m^3). This value was significantly higher compared to other months, since it exceeded 30 times the concentration in June. The polar plot revealed considerable Pb levels from south of the study site in January (Fig. 2C), where the main industrial sector of Bogota (Puente Aranda) is located at ~ 2.5 km (Fig. SD1). The greatest daily concentration of Pb was found on March 6 (1,481 ng/m^3), when the highest values of As (4.2 ng/m^3), Sb (67 ng/m^3), and Sn (28 ng/m^3) were also obtained (Fig. 1). The above suggests a common origin of these elements as industrial emissions.

Barium had the biggest monthly concentration in December-January (38 ng/m^3 - 43 ng/m^3; Table 2) and the largest daily concentration on March 11 (276 ng/m^3; Fig. 1). The polar plot of those months signaled

considerable values of Ba from S-SE at low wind speeds (< 1.2 m/s; Fig. 2D), possibly due to nearby sources such as exhaust and non-exhaust traffic emissions (Gietl et al., 2010; Peltier et al., 2011). Other origins of Ba, such as industrial emissions (González et al., 2014), are not discarded.

Fig. 3 shows the concentrations of the most abundant HMMP (Cu, Zn, Pb, and Ba) according to the days of the week. Copper and Pb had higher concentrations in weekends compared to weekdays (0.5% and 20%, respectively). This could suggest a predominantly stationary origin of these elements because several industries usually release emissions during weekends, when there are lower levels of air pollution in Bogota. Zinc and Ba showed a different trend, since their concentration was significantly lower during the weekends (45% and 34%, respectively). Taking into account that traffic is abruptly reduced on Sunday in this city, Zn and Ba could come from road traffic emissions.

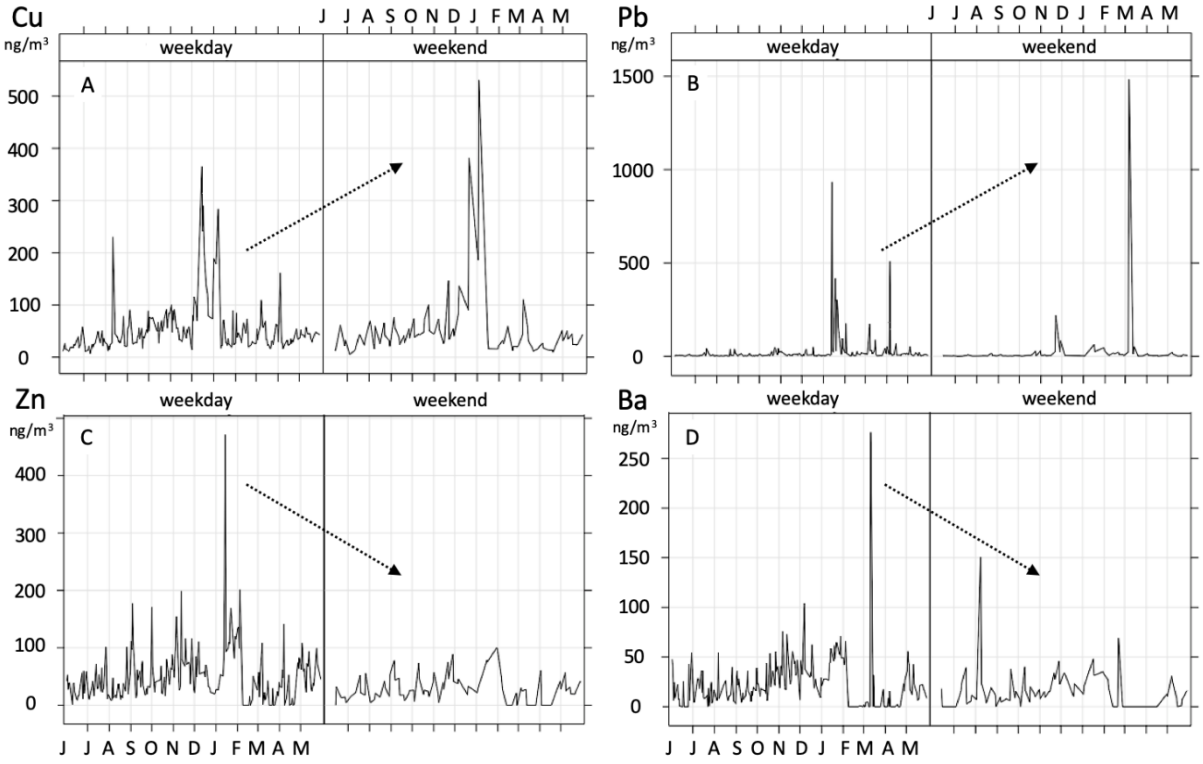

Fig. 3. Average concentrations of A) Cu, B) Pb, C) Zn, and D) Ba for weekdays as opposed to weekends.

3.3. Source analysis

3.3.1. Enrichment factors (EFs)

In order to identify the anthropogenic influence of the selected HMMP, EFs were calculated using Al as the reference element. Zinc, Pb, Sn, Cu, and Cd registered a moderate enrichment (10 < EFs < 100; Fig. 4), evidencing a significant influence of anthropogenic sources. Antimony was the only element

with a great enrichment (EF > 100), suggesting that this metalloid was mainly a result of human activities. The EF values of the carcinogenic elements such as Co, Cr, Ni, As, Pb, and Cd were 0.4, 0.9, 1.1, 3.2, 43 and 85, respectively. This shows that Pb and Cd proceeded predominantly from anthropogenic sources, while Co, Cr, Ni, and As originated from mixed sources.

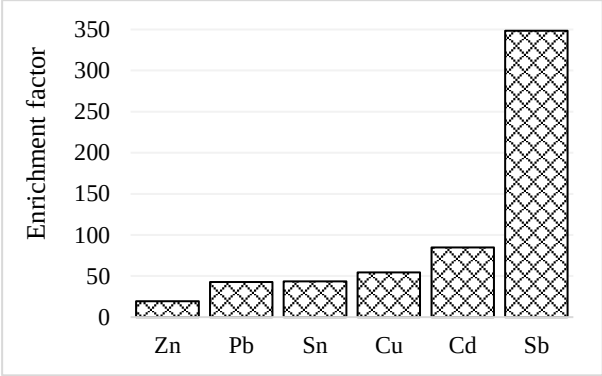

Fig. 4. Significant enrichment factors (EFs > 10) for the selected traces.

Zinc had a moderate correlation with Cr and Ba ($0.44 < r < 0.62$; Fig. SD2) indicating a common origin. These elements have been considered tracers of road dust (Zannoni et al., 2016), which is in line with studies of chemical composition of the thoracic fraction of road dust in Bogota (Ramírez et al., 2019). Zinc, Cr, and Ba have also been associated with exhaust emissions attributed to fuel and lubricant combustion (Peltier et al., 2011; Pulles et al., 2012).

Elements such as Pb, Sn, As, and Sb presented a moderate correlation with each other ($0.55 < r < 0.75$; Fig. SD2). These elements could come from commercial and industrial coal burning, since As and Pb have been considered tracers for coal combustion (Agarwal et al., 2017). Another plausible source is traffic-related emissions: Pb could be associated with wear of metal alloys and resuspension of road dust (Jaiprakash, 2017; Ramírez et al., 2019), Pb, Sb, and As with exhaust emissions from diesel vehicles (Pant and Harrison, 2013; Jaiprakash, 2017), and Pb, Sn, and Sb with brake wear (Amato et al., 2011; Grigoratos and Martini, 2014). The high level of Sb enrichment in the thoracic fraction stood out (EF = 348), similar to results obtained in Chinese cities such as Chengdu (Cheng et al., 2018). This metalloid is considered a priority air pollutant due to its deleterious effects on human health. Its sources have been related mainly to traffic and industrial emissions (e.g. smelters and waste incineration) in urban contexts (Sánchez-Rodas et al., 2017).

Cadmium, Zn, Co, As, and Sn had also a moderate correlation with each other ($0.40 < r < 0.75$; Fig. SD2). These elements may be associated with industrial sources, such as metallurgical sector and burning of fossil fuels (Suvarapu and Baek, 2017; Liu et al., 2018). The high level of Cd enrichment (EF = 85) supports this idea, since several studies have reported the main urban sources of Cd to be

anthropogenic. They include industrial (metal smelting, fossil fuel combustion, and waste incineration) (Cheng et al., 2018) and commercial activities (charcoal combustion) (Susaya et al., 2010), as well as exhaust emissions (Jaiprakash, 2017) and resuspension of road dust (Pant and Harrison, 2013; Ramírez et al., 2019). Copper did not show a statistically significant correlation with any other element, indicating the existence of a singular anthropic source.

3.3.2. Antimony speciation analysis

Speciation analysis of inorganic Sb was conducted considering the high enrichment factor of the metalloid. This analysis was performed to identify a potential association between Sb species and anthropogenic sources of PM, as previous studies have suggested (Sánchez-Rodas et al., 2017). A total of 14 samples with significant Sb concentration (higher than 4 ng/m^3) and a percentage of Sb extraction above 50% were analyzed. Table 3 shows the total Sb concentration, the amount of Sb(III), Sb (IV), and Sb extracted, and the distribution (in %) of Sb(III) and Sb(V) for each sample. The average concentration of Sb(III) was 1.6 ng/m^3, ranging between 0 - 8.7 ng/m^3, whereas Sb(V) had an average concentration of 12 ng/m^3, ranging from 2.4 ng/m^3 to 30 ng/m^3. The distribution of the Sb species revealed the predominance of Sb(V) over Sb(III) at the sampling site, with percentages of the pentavalent form between 78% and 100%. These values were higher than those registered in traffic stations in Granada, Spain (64-69%; Sánchez-Rodas et al., 2017) and Buenos Aires, Argentina (39-61%; Bellido-Martín et al., 2009), but they were similar to those found in industrial areas in Spain (85-86%; Sánchez-Rodas et al., 2017). The abundance of Sb(V) present in airborne PM has been reported in several megacities such as Tokyo and Ningbo (Iijima et al., 2010; Fang et al., 2019), even in similar proportions to those found in the current study (> 80%) (Zheng et al., 2000; Fang et al., 2019).

Table 3. Speciation of Sb contained in PM_{10} samples at an urban background site in Bogota. Concentrations in average ± standard deviation. Sb extracted corresponds to the sum of Sb(III) and Sb(V).

n	Date	Sb total (ng/m^3)	Sb(III) (ng/m^3)	Sb(V) (ng/m^3)	Sb extracted (ng/m^3)	Sb extracted (%)	Sb(III) (%)	Sb(V) (%)
1	06/04/2015	4.8	0.0	2.4	2.4	50	0	100
2	08/22/2015	11	0.0	5.8	5.8	53	0	100
3	08/26/2015	15	1.1	11	12	85	9	91
4	10/06/2015	6.1	0.6	5.4	6.0	98	10	90
5	10/23/2015	16	1.5	9.8	11	69	13	87
6	11/04/2015	42	1.8	24	26	60	7	93
7	11/28/2015	11	0.8	6.1	6.9	61	12	88
8	01/28/2016	23	2.0	19	21	91	10	90
9	02/02/2016	43	1.3	20	22	50	6	94
10	02/18/2016	11	1.7	8.4	10	92	17	83
11	03/02/2016	17	1.1	14	15	93	7	93
12	03/06/2016	67	8.7	30	39	58	22	78
13	04/14/2016	7.7	1.0	4.1	5.1	66	20	80
14	05/03/2016	6.9	0.3	3.8	4.1	60	7	93
	Total	20±18	1.6±2.1	12±8.6	13±10	71±17	10±6.5	90±6.5

Previous research has found that airborne PM_{10} collected at an industrial district had a higher Sb(V) proportion than that collected in traffic areas (Sánchez-Rodas et al., 2017), and PM_{10} collected at a traffic site had comparable or even higher Sb(III) concentrations than Sb(V) (Marconi et al., 2011; Quiroz et al., 2013). Therefore, the results obtained in the current study suggest that the study area was predominantly influenced by Sb(V) from industrial emissions. This can be explained by the proximity of the sampling site to two major industrial zones of the city (Puente Aranda and Fontibon, Fig. SD1), where Sb sources such as electroplating industry (Cheng et al., 2018), fuel combustion, and non-ferrous metals (Zhou et al., 2015) are located.

3.3.3. PMF analysis

In this study, PMF analysis was performed using all selected HMMP (eleven species in total). PMF model base run from three to eight factors to examine the optimal number of factors. The Q_{robust}/Q_{theory} value dropped maximally when factors changed from three to six (36%), suggesting that six factors would be necessary to explain the input data. The Q_{robust}/Q_{theory} values of the three- to eight-factor solution are shown in Fig. SD3. A good fit of the data is characterised by close values between Q_{robust} and Q_{theory} (JRC, 2019). The best proximity of these values was reached for six factors (Q_{robust}/Q_{theory} = 1.12), obtaining scaled residuals symmetrically distributed within a range of ±3 (Fig. SD4). Thus, six main sources of trace HMMP in PM_{10} were identified: fuel combustion and crustal dust, road dust, traffic-related emissions, copper smelting, iron and steel industry, and unidentified industry (Fig. 5).

The first factor is characterized by levels of Zn, Ba, Cu, Pb, Cr, Ni, and Sn, as well as significant contributions of Co (74%) and Ni (66%), followed by As (48%), Cr (48%), Zn (46%), and Ba (41%) (Fig. 5). Cobalt, Ni, As, and Pb have been considered typical elements for coal and oil combustion (Hsu et al., 2016; Hao et al., 2018). Vanadium is a key tracer of fuel combustion (Hao et al., 2018), therefore this element was added to the PMF model and a new analysis was carried out, revealing that this factor contributes 94% of V (Fig. SD5). Amounts of Cr, Zn, Ba, and Sn have also been associated with fuel combustion sources (Duan and Tan, 2013; Liu et al., 2018), supporting the denomination of the factor. The study area is ~ 2.5 km from two major industrial zones of the city (Puente Aranda and Fontibon; Fig. SD1), where a petrochemical complex and hundreds of industrial smokestacks are located. 20% of the industry uses coal and fuel oil, and 75% of commercial activities (including restaurants and street food stalls) regularly use charcoal as fuel (Pachón et al., 2018). Factor 1 had a higher contribution in dry season (January 2016, particularly; Fig. SD6), which can be explained by barbecue charcoal combustion, since it is an important source of Zn, Pb, Ba, Cu, V, Cr, and Co (Susaya et al., 2010), and the occurrence of local and regional forest fires, which release traces such as Zn, Pb, Co, Cu, Cr, and Ba (Alves et al., 2011; Odigie and Flegal, 2014). Enrichment factors of As, Co, Cr, Ni, and Ba were not significant (EFs < 10), hence a natural origin of these elements, as crustal dust, could be considered.

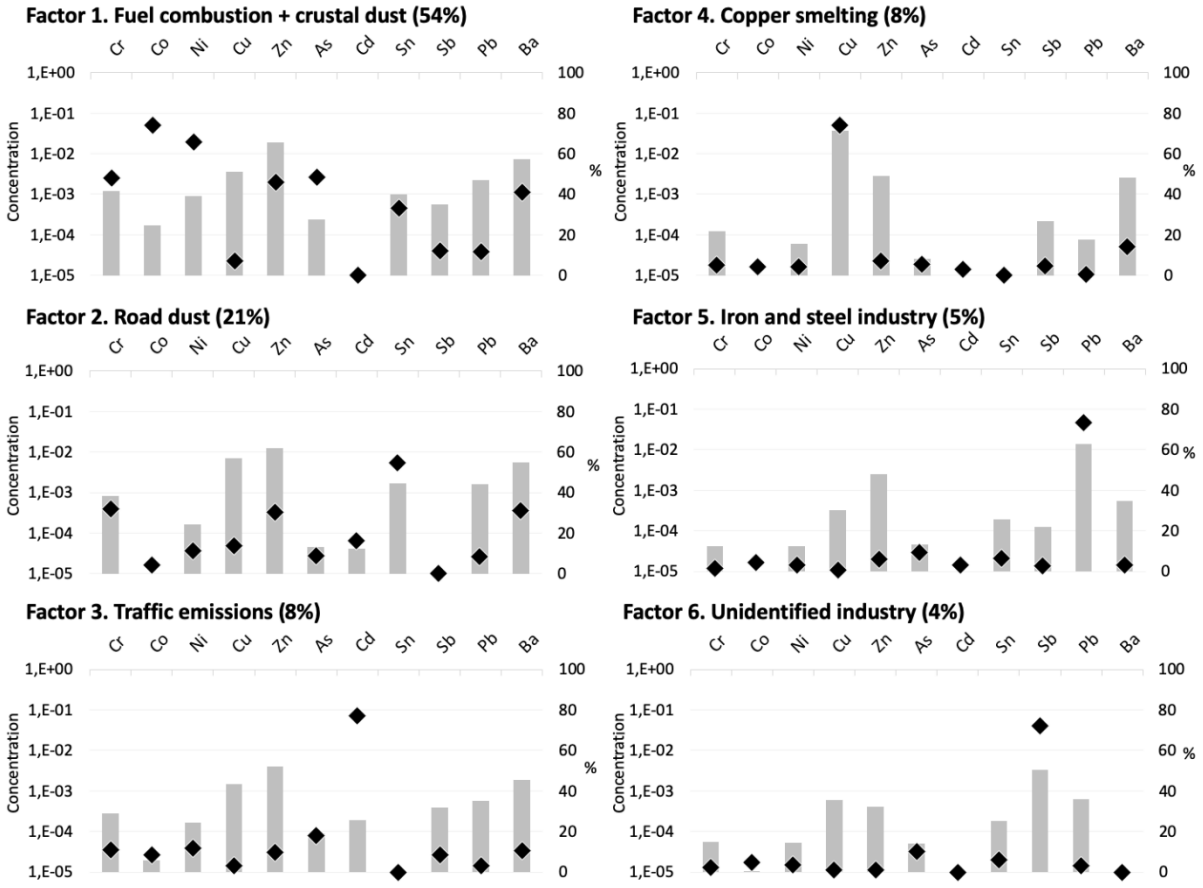

Fig. 5. Profiles of six sources identified for metals and metalloids particles in PM_{10} by PMF model.

The second factor is dominated by concentrations of Zn, Cu, Ba, Pb, Sn, and Cr, and high contributions of Sn (55%), Cr (32%), Ba (31%), and Zn (30%) (Fig. 5). Road dust is a mix of crustal material and anthropogenic particles emitted by traffic and stationary sources (Pant and Harrison, 2013). Trace elements such as Zn, Cu, Pb, and Sn showed a relevant enrichment factor (EF > 10). Numerous studies have associated amounts of Cu, Zn, Sn, and Pb with brake abrasion (Amato et al., 2011; Liu et al., 2018), tire wear (Lin et al., 2015; Hao et al., 2018) and wear of metal alloys (Jaiprakash, 2017). The enrichment of road dust with Pb, Ni, Cu, and Zn originating from industrial (Dall'Osto et al., 2013) or exhaust emissions (Cong et al., 2011) is not excluded, as was suggested by recent studies in Bogota (Ramírez et al., 2019). Concentrations of traces with EF < 10, such as Cr and Ba, is consistent with the denomination of this factor, since they could come from both material crustal (Hsu et al., 2016) and traffic-related emissions (Harrison et al., 2012; Lin et al., 2015). The second factor registered a slight increase during a dry season (January 2016; Fig. SD6), which could be related to a higher accumulation and resuspension of road dust.

The third factor is integrated by Zn, Cu, Ba, Pb, Sb, and Cr, as well as important contributions of Cd (77%; Fig. 5). Traffic-related emissions, including exhaust and non-exhaust, are characterized by high

amounts of these elements (Hsu et al., 2016; Hao et al., 2018). Zinc and Cu are commonly-used tracers for vehicle exhaust (Zhang et al., 2017; Hao et al., 2018). Elements such as Zn, Cr, Sb, Ba, Pb, Ni, Co, Cd, and Cu have been associated with tailpipe emissions, comprising the composition of fuel and lubricant oil (Lin et al., 2015; Jaiprakash, 2017; Liu et al., 2018; Wang et al., 2018b). The high contribution of Cd and amounts of Pb, Cu, Ba, Sb, Cr, and Zn suggest non-exhaust emissions (Thorpe and Harrison, 2008). Studies conducted in China have reported that Cd is mostly emitted by tire wear source in cities (Zhao et al., 2019). The third factor had the highest contributions in a rainy period (November 2015; Fig. SD6), which is consistent with its denomination, as previous studies have reported that the use of vehicles increases during rainy seasons in Bogota, and with it the variability of traffic speed, acceleration and braking rates (Ramírez et al., 2018a).

The fourth factor is characterized by high contribution of Cu (74%) and amounts of Zn and Ba (Fig. 5). Previous studies have identified Cu and Zn as key tracers for copper smelters (González et al., 2014; Chen et al., 2016). Barium has been recognized to be one of the first order elements associated with copper smelting (Valdés et al., 2013). The presence of Pb and As is consistent with the denomination of this factor. Although there is no detailed inventory of Cu-smelter industries in Bogota, official data report more than 100 non-ferrous metals smelting located south of the city (CCB, 2016), particularly copper and bronze industry according to the International Standard Industrial Classification - ISIC (UN, 2008). The temporal variability of this factor (Fig. SD6) and higher levels of Cu in weekends compared to weekdays (Fig. 3) are consistent with a stationary source.

The fifth factor is characterized by a high contribution of Pb (73%) and levels of Zn (Fig. 5). Lead and Zn have been recognized as key trace elements attributed to steel industry (Geagea et al., 2007; Beddows and Harrison, 2018). They are emitted by basic oxygen steelmaking (Dall'Osto et al., 2008; Almeida et al., 2015) and could be emitted as impurities in metal ores or as smelting agents (Hao et al., 2018). Since Fe is a key tracer of steel industry (Beddows and Harrison, 2018), a new PMF run was carried out including this metal. Fig. SD7 shows that this factor has significant concentrations of Fe, supporting the denomination of this factor. According to the ISIC (UN, 2008), there are more than 40 industries of iron and steel casting in Bogota, most of them located south of the city (CCB, 2016). The sporadic behavior of this factor (Fig. SD6) and higher levels of Pb during the weekends (Fig. 3) are consistent with an industrial source. Emissions of Pb from other industrial activities such as smelting, alloys production, and paint manufacturing are not discarded (Colnodo et al., 2016; Gope et al., 2018).

The sixth factor is dominated by high contributions of Sb (72%) and concentrations of others traces such as Cu, Pb, and Zn (Fig. 5). The irregular temporal contribution of this factor (Fig. SD6) and the Sb speciation results suggest an industrial source. Electroplating industry is a sector with significant emissions of Sb (Cheng et al., 2018). Although there is not an updated inventory of these types of

industries in Bogota, it is known that the city concentrates most of these activities in Colombia (SDA, 2010). Other industries identified as sources of Sb are fuel combustion, non-ferrous metals, production of textile and plastic, and waste incineration (Zhou et al., 2015; Li et al., 2019). Contributions of Cu, Pb, Zn, and Sb from traffic emissions could enrich this factor. It is not possible to clearly name the sixth factor with the available data.

Finally, the results indicated that fuel combustion and crustal dust (Factor 1) were the major sources of Cr, Co, Ni, Zn, As, and Ba (Fig. 6). Road dust (Factor 2) was the main cause for Cu, traffic emissions (Factor 3) for Sn, copper smelting (Factor 4) for Pb, iron and steel industry (Factor 5) for Cd, and an unidentified industrial sector (Factor 6) was the main source of Sb.

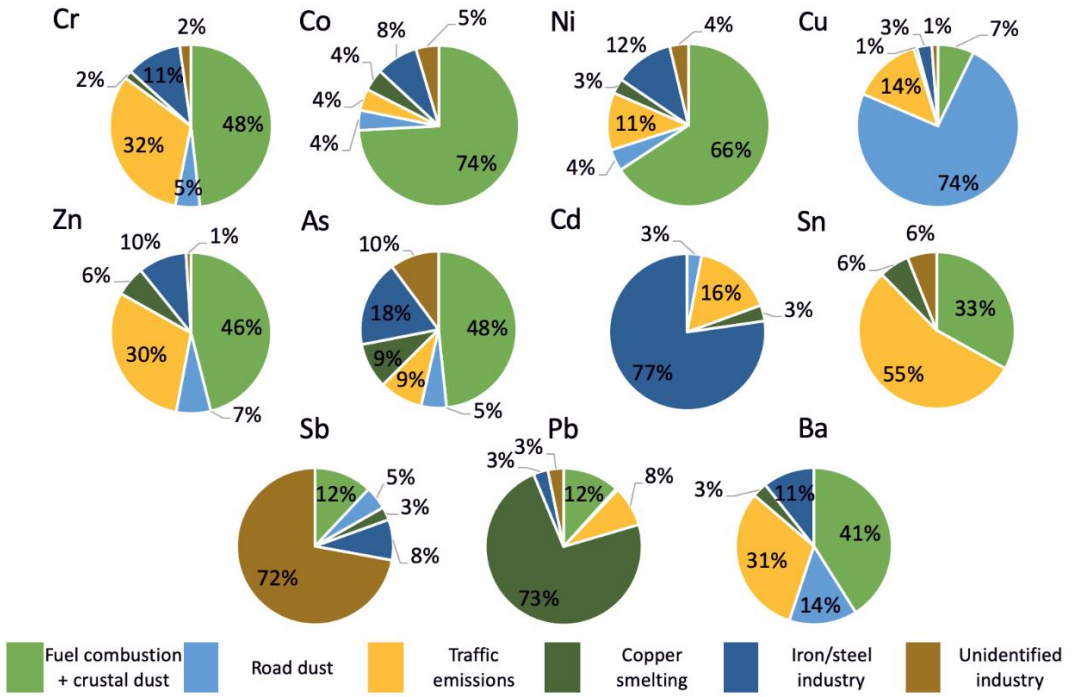

Fig. 6. Mean source contribution to selected heavy metals and metalloids in PM_{10}.

3.4. Health risk assessment

A health risk assessment was conducted for seven carcinogens using the mean concentration of each element in PM_{10} and equations 3 and 4. Lead had the highest exposure concentration for both children and adults (Table 4). The cancer risk was $< 1 \times 10^{-6}$ for inhalation exposure to Co, Ni, As, Cd, Sb(III), and Pb, indicating that the risk was negligible for the two populations considered at the sampling site (Table 4). However, the value of adjusted Cr(VI) was slightly higher than the minimum acceptable risk level for adults, considering the entire study period (1.4×10^{-6}). This means that adjusted Cr(VI) may pose risk in a near future, which is in line with previous studies conducted in greatly populated Asian cities, such as Agra (Sah et al., 2019), Beijing (Gao and Ji, 2018), Baotou (Li et al., 2016a), Delhi

(Khillare and Sarkar, 2012), and Nanjing (Li et al., 2016b). Therefore, control measures should be focused on the emission sources of this metal, such as fuel combustion and traffic emissions (Fig. 6), as well as metallurgy industry, electroplating, and production of paints, pigments, pulp, and paper (Jaishankar et al., 2014). The average risk values for both adults and children decreased in the following order: adjusted Cr(VI) > Co > As > Sb(III) > Cd > Ni > Pb.

Table 4. Carcinogenic risks from toxic metals and metalloids via inhalation exposure to PM_{10}. Exposure concentration (ExpC) was calculated using Eq. 3.

Element	ExpC (ng/m^3)		Carcinogenic risk	
	Children	Adults	Children	Adults
Cr(VI)	0.03	0.12	3.5×10^{-7}	1.4×10^{-6}
Co	0.02	0.07	1.3×10^{-7}	5.3×10^{-7}
Ni	0.12	0.48	2.9×10^{-8}	1.1×10^{-7}
As	0.04	0.15	1.2×10^{-7}	4.9×10^{-7}
Cd	0.02	0.07	3.3×10^{-8}	1.3×10^{-7}
Sb(III)	0.11	0.45	7.9×10^{-8}	3.2×10^{-7}
Pb	1.76	7.03	2.1×10^{-8}	8.4×10^{-8}
Sum	2.09	8.36	7.7×10^{-7}	3.1×10^{-6}

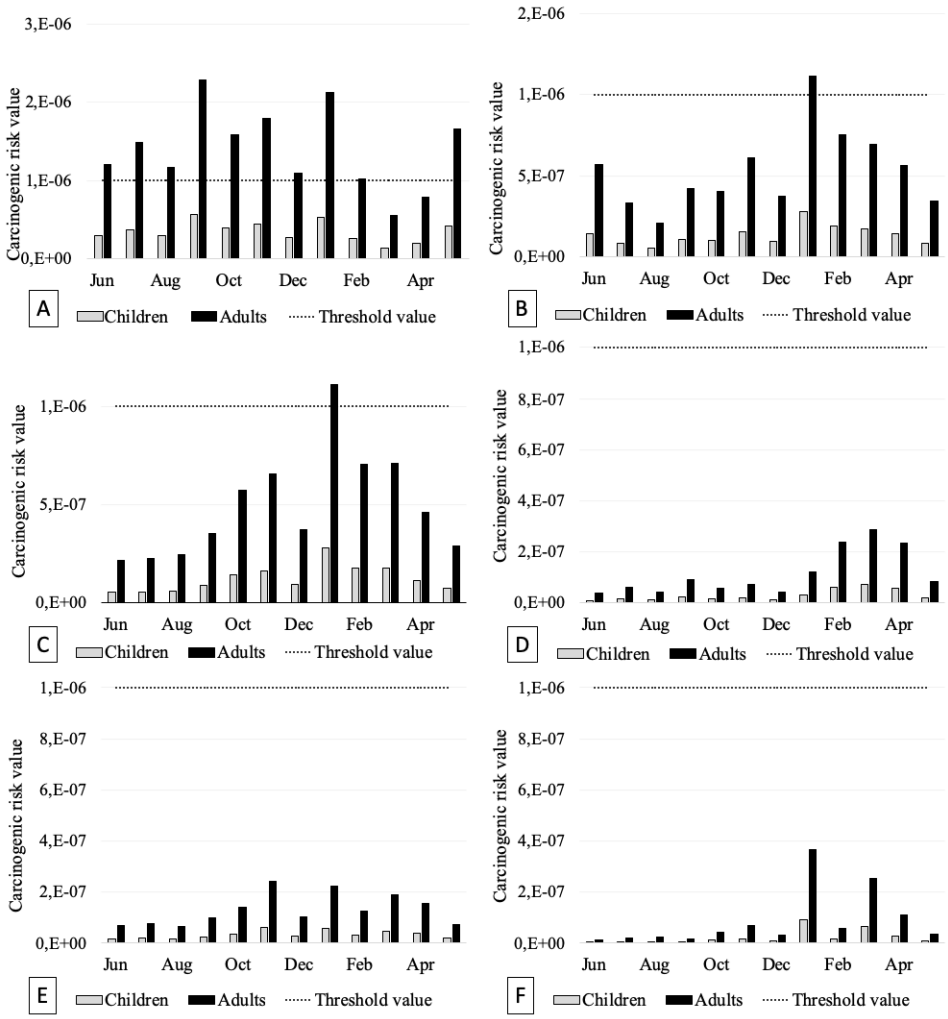

Fig. 7. Monthly variations of cancer risk values for the inhalation of A) adjusted Cr(VI), B) Co, C) As, D) Ni, E) Cd, and F) Pb in PM_{10}, for both children and adults.

The monthly cancer risk was calculated for the carcinogens, observing that only adjusted Cr(VI), Co, and As exceeded the minimum threshold value (Fig. 7). January stood out because it presented the highest carcinogenic risk values (1.1×10^{-6}) for Co and As. September and January recorded the highest values for adjusted Cr(VI) with a cancer risk two orders of magnitude higher than the minimum threshold value (2.3×10^{-6} and 2.1×10^{-6}, respectively). It was observed that the sum of cancer risk in adults (3.1×10^{-6}) via inhalation was greater than in children (7.7×10^{-7}), which is in line with previous studies (Sun et al., 2014; Sah et al., 2019). This implies that for every million adults three may get cancer from exposure to toxic HMMP via inhalation of PM_{10} in a lifetime. This value is not critical because it does not exceed the maximum threshold, but it should not be underestimated considering that the sampling was taken at an urban background site.

4. Conclusions

Copper, Zn, Pb, and Ba were the trace metals with the highest concentrations in the thoracic fraction. Most of the selected metals and metalloids had higher levels in the dry season (January to March), characterized by recurrent local and regional forest fires, and BBQ charcoal combustion particularly during the first half in January. Concentrations of Cu and Pb were higher during weekends than weekdays, which could be associated with industrial emissions. Meanwhile, Zinc and Ba presented lower concentrations during weekends compared to weekdays, suggesting an association with road traffic emissions. Zinc, Pb, Sn, Cu, and Cd registered an enrichment factor > 10, indicating a strong influence of anthropogenic sources. Antimony had the highest enrichment factor (EF = 348), stating an anthropogenic origin. Antimony speciation analysis revealed that Sb(V) was the main species present in the PM_{10} fraction (> 80%) with a predominant industrial origin. The major sources of trace metals and metalloids particles were fuel combustion and crustal dust, road dust, traffic-related emissions, copper smelting, iron and steel industry, and an unidentified industrial sector. The first two sources stood out since they explained 75% of the PM_{10} mass. None of the carcinogens analyzed posed a significant cancer risk at the study site. For children, carcinogenic risks because of exposure to adjusted Cr(VI), Co, Ni, As, Cd, Sb(III), and Pb were all lower than the accepted risk level (1×10^{-6}). However, adjusted Cr(VI) slightly exceeded the minimum threshold value for adults. The results of this study can help environmental and health authorities, as well as policy makers, to recognize the characteristics of anthropogenic thoracic particles to guide control strategies towards the critical emission sources.

Acknowledgments

The authors would like to thank the Universidad Internacional de Andalucía (UNIA) and the Regional Council for the Environment of the Junta de Andalucía for partially funding this project. Thanks are also

due to the R and OpenAir Projects, and to the District Department of the Environment of Bogota (SDA) for meteorological data.

Appendix A. Supplementary data

Supplementary data to this article can be found online at

References

Agarwal, A., Mangal, A., Satsangi, A., Lakhani, A., Kumari, K., 2017. Characterization, sources and health risk analysis of $PM_{2.5}$ bound metals during foggy and non-foggy days in sub-urban atmosphere of Agra. Atmos. Res. 197, 121-131.

Albuquerque, M., Coutinho, M., Rodrigues, J., Ginja, J., Borrego, C., 2017. Long-term monitoring of trace metals in PM_{10} and total gaseous mercury in the atmosphere of Porto, Portugal. Atmos. Pollut. Res. 8, 535-544.

Almeida, S., Lage, J., Fernández, B., Garcia, S., Reis, M., Chaves, P., 2015. Chemical characterization of atmospheric particles and source apportionment in the vicinity of a steelmaking industry. Sci. Total Environ. 521-522, 411-420.

Alves, C., Vicente, A., Nunes, T., Gonçalves, C., Fernandes, A., Mirante, F., Tarelho, L., Sánchez de la Campa, A.M., Querol, X., Caseiro, A., Monteiro, C., Evtyugina, M., Pio, C., 2011. Summer 2009 wildfires in Portugal: emission of trace gases and aerosol composition. Atmos. Environ. 45(3), 641-649.

Amato, F., Pandolfi, M., Moreno, T., Furger, M., Pey, J., Alastuey, A., Bukowiecki, N., Prevot, A., Baltensberger, U., Querol, X. 2011. Sources and variability of inhalable road dust particles in three European cities. Atmos. Environ. 45, 6777-6787.

Amato, F., Pandolfi, M., Escrig, A., Querol, X., Alastuey, A., Pey, J., Perez, N., Hopke, P.K., 2009. Quantifying road dust resuspension in urban environment by Multilinear Engine: a comparison with PMF2. Atmos. Environ. 43, 2770-2780.

Apeagyei, E., Bank, M., Spengler, J., 2011. Distribution of heavy metals in road dust along an urban-rural gradient in Massachusetts. Atmos. Environ. 45, 2310-2323.

Beddows, D., Harrison, R., 2018. Identification of specific sources of airborne particles emitted from within a complex industrial (steelworks) site. Atmos. Environ. 183, 122-134.

Bell, M., Belanger, K., Ebisu, K., Gent, J., Lee, H., Koutrakis, P., Leaderer, B., 2010. Prenatal exposure to fine particulate matter and birth weight: variations by particulate constituents and sources. Epidemiology 21, 884-891.

Bellido-Martín, A., Gómez-Ariza, J., Smichowsky, P., Sánchez-Rodas, D., 2009. Speciation of antimony in airborne particulate matter using ultrasound probe fast extraction and analysis by HPLC-HG-AFS. Anal. Chim. Acta 649, 191-195.

CCB - Cámara de Comercio de Bogotá, 2016. Establecimientos comerciales, área urbana, Bogotá D.C. Bogotá, Cámara de Comercio de Bogotá. Obtained from https://mapas.bogota.gov.co (accessed 09 May 2019).

Cesari, D., De Benedetto, G., Bonasoni, P., Busetto, M., Dinoi, A., Merico, E., Chirizzi, D., Cristofanelli, P., Donateo, A., Grasso, F., Marinoni, A., Pennetta, A., Contini, D., 2018. Seasonal variability of $PM_{2.5}$ and PM_{10} composition and sources in an urban background site in Southern Italy. Sci. Total Environ. 612, 202-213.

Chandra, S., Kulshrestha, M., Singh, R., Singh, N., 2017. Chemical characteristics of trace metals in PM_{10} and their concentrated weighted trajectory analysis at Central Delhi, India. J. Environ. Sci. 55, 184-196.

Chen, B., Stein, A., Castell, N., Gonzalez-Castanedo, Y., Sánchez de la Campa, A.M., de la Rosa, J., 2016. Modeling and evaluation of urban pollution events of atmospheric heavy metals from a large Cu-smelter. Sci. Total Environ. 539, 17-25.

Cheng, X., Huang, Y., Zhang, Sh., Ni, Sh., Long, Z., 2018. Characteristics, sources, and health risk assessment of trace elements in PM_{10} at an urban site in Chengdu, Southwest China. Aerosol Air Qual. Res. 18, 357-370.

Colnodo, RDS, IPEN, 2016. Plomo en pinturas a base de solventes para uso doméstico en Colombia. Bogotá, Colnodo/Red de Desarrollo Sostenible.

Cong, Z., Kang, Sh., Luo, Ch., Li, Q., Huang, J., Gao, Sh., Li, X., 2011. Trace elements and lead isotopic composition of PM_{10} in Lhasa, Tibet. Atmos. Environ. 45, 6210-6215.

Councell, T., Duckenfield, K., Landa, E., Callender, E., 2004. Tire-wear particles as a source of zinc to the environment. Environ. Sci. Technol. 38, 4206-4214.

Crilley, L., Lucarelli, F., Bloss, W., Harrison, R., Beddows, D., Calzolai, G., Nava, S., Valli, G., Bernardoni, V., Vecchi, R., 2017. Source apportionment of fine and coarse particles at a roadside and urban background site in London during the 2012 summer ClearfLo campaign. Environ. Pollut. 220, 766-778

Dallmann, T., Onasch, T., Kirchstetter, T., Worton, D., Fortner, E., Herndon, S., Wood, E., Franklin, J., Worsnop, D., Goldstein, A., Harle, R., 2014. Characterization of particulate matter emissions from on-road gasoline and diesel vehicles using a soot particle aerosol mass spectrometer. Atmos. Chem. Phys. 14, 7585-7599.

Dall'Osto, M., Querol, X., Amato, F., Karanasiou, A., Lucarelli, F., Nava, S., Calzolai, G., Chiarim, M., 2013. Hourly elemental concentrations in $PM_{2.5}$ aerosols sampled simultaneously at urban background and road site during SAPUSS - diurnal variations and PMF receptor modelling. Atmos. Chem. Phys. 13, 4375-4392.

Dall'Osto, M., Booth, M., Smith, W., Fisher, R., Harrison, R., 2008. A study of the size distributions and the chemical characterization of airborne particles in the vicinity of a large integrated steelworks. Aerosol Sci. Technol. 42, 981-991.

DANE - Departamento Administrativo Nacional de Estadística, 2010. Proyecciones nacionales y departamentales de población 2005-2020. Bogotá, DANE.

Demographia, 2019. Demographia World Urban Areas. 15th annual edition. http://demographia.com/db-worldua.pdf (accessed 25 April 2019).

Dodge, D., Silva, R., 2019. Cobalt and cobalt compounds cancer Inhalation Unit Risk factors. Technical support document for cancer potency factors Appendix B. California Environmental Protection Agency.

Duan, J., Tan, J., 2013. Atmospheric heavy metals and Arsenic in China: situation, sources and control policies. Atmos. Environ. 74, 93-101.

Fang, L., Zhang, Y., Lu, B., Wang, L., Yao, X., Ge, T., 2019. New two-step extraction method in antimony speciation using HPLC-ICP-MS technique in inhalable particulate matter ($PM_{2.5}$). Microchem. J. 146, 1269-1275.

Filella, M., Belzile, N., Chen, Y.W., 2002. Antimony in the environment: a review focused on natural waters I. Occurrence. Earth-Sci. Rev. 57, 125-176.

Franklin, M., Koutrakis, P., Schwartz, J., 2008. The role of particle composition on the association between $PM_{2.5}$ and mortality. Epidemiology 19, 680-689.

Gao, Y., Ji, H., 2018. Microscopic morphology and seasonal variation of health effect arising from heavy metals in $PM_{2.5}$ and PM_{10}: one-year measurement in a densely populated area of urban Beijing. Atmos. Res. 212, 213-226.

Geagea, L., Stille, P., Millet, M., Perrone, Th., 2007. REE characteristics and Pb, Sr and Nd isotopic compositions of steel plant emissions. Sci. Total Environ. 373, 404-419.

Gehring, U., Beelen, R., Eeftens, M., Hoek, G., de Hoogh, K., de Jongste, J.C., Keuken, M., Koppelman, G.H., Meliefste, K., Oldenwening, M., Postma, D.S., van Rossem, L., Wang, M., Smit, H.A., Brunekreef, B., 2015. Particulate matter composition and respiratory health: the PIAMA birth cohort study. Epidemiology 26, 300-309.

Gietl, J., Lawrence, R., Thorpe, A., Harrison, R., 2010. Identification of brake wear particles and derivation of a quantitative tracer for brake dust at a major road. Atmos. Environ. 44 (2), 141-146.

González, Y., Moreno, T., Fernández, R., Sánchez de la Campa, A., Alastuey, A., Querol, X., de la Rosa, J., 2014. Size distribution and chemical composition of particulate matter stack emissions in and around a copper smelter. Atmos. Environ. 98, 271-282.

Gope, M., Masto, R., George, J., Balachandran, S., 2018. Tracing source, distribution and health risk of potentially harmful elements (PHEs) in street dust of Durgapur, India. Ecotoxicol. Environ. Saf. 154, 280-293.

Green, J., Sánchez, S., 2013. Air quality in Latin America: an overview. Washington D.C., Clean Air Institute.

Grigoratos, T., Martini, G., 2014. Non-exhaust traffic related emissions. Brake and tyre wear PM. Literature Review. Luxembourg, Joint Research Centre.

Hao, Y., Meng, X., Yu, X., Lei, M., Li, M., Shi, F., Yang, W., Zhang, Sh., Xie, Sh., 2018. Characteristics of trace elements in $PM_{2.5}$ and PM_{10} of Chifeng, northeast China: insights into spatiotemporal variations and sources. Atmos. Res. 213, 550-561.

Harrison, R., Jones, A., Gietl, J., Yin, J., Green, D., 2012. Estimation of the contributions of brake dust, tire wear, and resuspension to nonexhaust traffic particles derived from atmospheric measurements. Environ. Sci. Technol. 46, 6523-6529.

He, M., Wang, N., Long, X., Zhang, Ch., Ma, C., Zhong, Q., Wang, A., Wang, Y., Pervaiz, A., Shan, J., 2019. Antimony speciation in the environment: Recent advances in understanding the biogeochemical processes and ecological effects. J. Environ. Sci. 75, 14-39.

Hernández, L., Aristizabal, G., Quiroz, L., Medina, K., Rodríguez, N., Sarmiento, R., Osorio, S., 2013.

687 Air pollution and respiratory illness in children aged less than 5 years-old in Bogota, 2007. Rev. salud
688 pública 15(4), 503-516.
689
690 Hieu, N., Lee, B., 2010. Characteristics of particulate matter and metals in the ambient air from a
691 residential area in the largest industrial city in Korea. Atmos. Res. 98, 526-537.
692
693 Hsu, Ch., Chiang, H., Lin, S., Chen, M., Lin, T., Chen, Y., 2016. Elemental characterization and source
694 apportionment of PM_{10} and $PM_{2.5}$ in the western coastal area of central Taiwan. Sci. Total Environ. 541,
695 1139-1150.
696
697 IARC- International Agency for Research on Cancer, 2016. Outdoor air pollution, Volume 109. Lyon,
698 WHO.
699
700 IARC, 2012. Arsenic, metals, fibres and dusts. A review of human carcinogens. Volume 100C. Lyon,
701 WHO.
702
703 IARC, 2006a. Cobalt in hard metals and Cobalt Sulfate, Gallium Arsenide, Indium Phosphide and
704 Vanadium Pentoxide. Volume 86. Lyon, France: WHO.
705
706 IARC, 2006b. Inorganic and Organic Lead Compounds. Volume 87. Lyon, WHO.
707
708 IARC, 1990. Chromium (III) compounds. Volume 49. Lyon, WHO.
709
710 IARC, 1989. Antimony Trioxide and Antimony Trisulfide. Volume 47. Lyon, WHO.
711
712 IDEAM - Instituto de Hidrología, Meteorología y Estudios Ambientales, 2016. Informe del estado de la
713 calidad del aire en Colombia 2011 - 2015. Bogotá, Ministerio de Ambiente y Desarrollo Sostenible.
714
715 IHME - Institute for Health Metrics and Evaluation, 2017. State of global air. A special report on global
716 exposure to air pollution and its disease burden. Boston, Health Effects Institute.
717
718 Iijima, A., Sato, K., Ikeda, T., Sato, H., Kozawa, K., Furuta, N., 2010. Concentration distributions of
719 dissolved Sb(III) and Sb(V) species in size-classified inhalable airborne particulate matter. J. Anal. At.
720 Spectrom. 25, 356-363.
721
722 Jaiprakash, G., 2017. Chemical and optical properties of $PM_{2.5}$ from on-road operation of light duty
723 vehicles in Delhi city. Sci. Total Environ. 586, 900-916.
724
725 Jaishankar, M., Tseten, T., Anbalagan, N., Mathew, B., Beeregowda, K., 2014. Toxicity, mechanism
726 and health effects of some heavy metals. Interdiscip. Toxicol. 7(2), 60-72.
727
728 Jena, S., Singh, G., 2017. Human health risk assessment of airborne trace elements in Dhanbad, India.
729 Atmos. Pollut. Res. 8, 490-502.
730
731 Jin, L., Xie, J., Wong, C., Chan, S., Abbaszade, G., Schnelle-Kreis, J., Zimmermann, R., Li, J.,
732 Zhang, G., Fu, P., Li, X., 2019. Contributions of city-specific fine particulate matter ($PM_{2.5}$) to
733 differential in vitro oxidative stress and toxicity implications between Beijing and Guangzhou of China.
734 Environ. Sci. Technol. 53 (5), 2881-2891.
735
736 JRC - Joint Research Centre, 2019. European guide on air pollution source apportionment with receptor
737 models. Revision 2019.
738
739 Kabir, E., Kim, K., Yoon, H., 2011. Trace metal contents in barbeque (BBQ) charcoal products. J.
740 Hazard. Mater. 185, 1418-1424.
741

Khillare, P., Sarkar, S., 2012. Airborne inhalable metals in residential areas of Delhi, India: distribution, source apportionment and health risks. Atmos. Pollut. Res. 3, 46-54.

Lelieveld, J., Klingmüller, K., Pozzer, A., Pöschl, U., Fnais, M., Daiber, A., Münzel, T., 2019. Cardiovascular disease burden from ambient air pollution in Europe reassessed using novel hazard ratio functions. Eur. Heart J. 0, 1-7.

Li, Y., Zhang, H., Shao, L., Zhou, X., He, P., 2019. Impact of municipal solid waste incineration on heavy metals in the surrounding soils by multivariate analysis and lead isotope analysis. J. Environ. Sci. 82, 47-56.

Li, K., Liang, T., Wang, L., 2016a. Risk assessment of atmospheric heavy metals exposure in Baotou, a typical industrial city in northern China. Environ. Geochem. Health 38, 843-853.

Li, H., Wang, Q., Shao, Sh., Wang, J., Wang, Ch., Sun, Y., Qian, X., Wu, H., Yang, M., Li, F., 2016b. Fractionation of airborne particulate-bound elements in haze-fog episode and associated health risks in a megacity of southeast China. Environ. Pollut. 208, 655-662.

Lin, Y., Tsai, C., Wu, Y., Zhang, R., Chi, K., Huang, Y., Lin, S., Hsu, S., 2015. Characteristics of trace metals in traffic-derived particles in Hsuehshan Tunnel, Taiwan: size distribution, potential source, and fingerprinting metal ratio. Atmos. Chem. Phys. 15, 4117-4130.

Liu, Y., Xing, J., Wang, Sh., Fu, X., Zheng, H., 2018. Source-specific speciation profiles of $PM_{2.5}$ for heavy metals and their anthropogenic emissions in China. Environ. Pollut. 239, 544-553.

Marconi, E., Canepari, S., Astolfi, M., Perrino, C., 2011. Determination of Sb(III), Sb(V) and identification of Sb-containing nanoparticles in airborne particulate matter. Procedia Environ. Sci. 4, 209-217.

Molina, L., Molina, M., Slott, R., Kolb, C., Gbor, P., Meng, F., Singh, R., Galvez, O., Sloan, J., Anderson, W., Tang, X., Shao, M., Zhu, T., Zhang, Y., Hu, M., Gurjar, B., Artaxo, P., Oyola, P., Gramsch, E., Hidalgo, P., Gertler, A., 2004. Air quality in selected megacities. J. Air Waste Manag. Assoc. 54:12, 1-73.

Moreno, T., Querol, X., Alastuey, A., Viana, M., Salvador, P., de la Campa A.M., Artiñano, B., de la Rosa, J., Gibbons, W., 2006. Variations in atmospheric PM trace metal content in Spanish towns: illustrating the chemical complexity of the inorganic urban aerosol cocktail. Atmos. Environ. 40, 6791-6803.

Muránszky, G., Óvári, M., Virág, I., Csiba, P., Dobai, R., Záray, G., 2011. Chemical characterization of PM_{10} fractions of urban aerosol. Microchem. J. 98, 1-10.

National Research Council, 2000. Toxicological risks of selected flame-retardant chemicals. Washington D.C., Subcommittee on Flame-Retardant Chemicals, Committee on Toxicology, Board on Environmental Studies and Toxicology.

Odigie, K., Flegal, A., 2014. Trace metal inventories and lead isotopic composition chronicle a forest fire's remobilization of industrial contaminants deposited in the Angeles National Forest. PLoS ONE 9(9), e107835.

Paatero, P., 1997. Least squares formulation of robust non-negative factor analysis. Chemom. Intell. Lab. Syst. 37, 23-35.

Paatero, P., Tapper, U., 1994. Positive matrix factorization: a non-negative factor model with optimal utilization of error estimates of data values. Environmetrics 5, 111-126.

Pachón, J., Galvis, B., Lombana, O., Carmona, L., Fajardo, S., Rincón, A., Meneses, S., Chaparro, R., Nedbor-Gross, R., Henderson, B., 2018. Development and evaluation of a comprehensive atmospheric emission inventory for air quality modeling in the megacity of Bogotá. Atmosphere 9(2), 49.

Pachón, J., Sarmiento H., 2008. Heavy metal determination and source emission identification in an industrial location of Bogota Colombia. Rev. Fac. Ing-Univ. Ant. 43, 120-133.

Pant, P., Harrison, R., 2013. Estimation of the contribution of road traffic emissions to particulate matter concentrations from field measurements: a review. Atmos. Environ. 77, 78-97.

Park, E., Kim, D., Park, K., 2008. Monitoring of ambient particles and heavy metals in a residential area of Seoul, Korea. Environ. Monit. Assess. 137, 441-449.

Pasha, M., Alharbi, B., 2015. Characterization of size-fractionated PM_{10} and associated heavy metals at two semi-arid holy sites during Hajj in Saudi Arabia. Atmos. Pollut. Res. 6, 162-172.

Peltier, R., Cromar, K., Ma, Y., Fan, Z., Lippmann, M., 2011. Spatial and seasonal distribution of aerosol chemical components in New York City: (2) road dust and other tracers of traffic-generated air pollution. J. Expo. Sci. Environ. Epidemiol. 21(5), 484-494.

Pérez, N., Pey, J., Reche, C., Cortés, J., Alastuey, A., Querol, X., 2016. Impact of harbor emissions on ambient PM_{10} and $PM_{2.5}$ in Barcelona (Spain): evidences of secondary aerosol formation within the urban area. Sci. Total Environ. 571, 237-250.

Pulles, T., van der Gon, H., Appelman, W., Verheul, M., 2012. Emission factors for heavy metals from diesel and petrol used in European vehicles. Atmos. Environ. 61, 641-651.

Querol, X., Alastuey, A., Moreno, T., Viana, M., Castillo, S., Pey, J., Rodríguez, S., Artiñano, B., Salvador, P., Sánchez, M., García Dos Santos, S., Herce Garraleta, M., Fernández-Partier, R., Moreno-Grau, S., Negral, L., Minguillón, M., Monfort, E., Sanz, M., Palomo-Marín, R., Pinilla-Gil, E., Cuevas, E., de la Rosa, J., Sánchez de la Campa, A., 2008. Spatial and temporal variations in airborne particulate matter (PM_{10} and $PM_{2.5}$) across Spain 1999-2005. Atmos. Environ. 42, 3964-3979.

Quiroz, W., Cortés, M., Astudillo, F., Bravo, M., Cereceda, F., Vidal, V., Lobos, M., 2013. Antimony speciation in road dust and urban particulate matter in Valparaiso, Chile: Analytical and environmental considerations. Microchem. J. 110, 266-272.

Ramírez, O., Sánchez de la Campa, A.M., Amato, F., Moreno, T., Silva, L., de la Rosa, J., 2019. Physicochemical characterization and sources of the thoracic fraction of road dust in a Latin American megacity. Sci. Total Environ. 652, 434-446.

Ramírez, O., Sánchez de la Campa, A.M., Amato, F., Catacolí, R., Rojas, N., de la Rosa, J., 2018a. Chemical composition and source apportionment of PM_{10} at an urban background site in a high-altitude Latin American megacity (Bogota, Colombia). Environ. Pollut. 233, 142-155.

Ramírez, O., Sánchez de la Campa, A.M., de la Rosa, J., 2018b. Characteristics and temporal variations of organic and elemental carbon aerosols in a high-altitude, tropical Latin American megacity. Atmos. Res. 210, 110-122.

Ramírez, O., Mura, I., Franco, J., 2017. How do people understand urban air pollution? Exploring citizens' perception on air quality, its causes and impacts in Colombian cities. Open J. Air Pollut. 6, 1-17.

Rudnick, R., Gao, S., 2003. Composition of the continental crust. Treatise on Geochemistry 3, 1-64.

Sah, D., Kumar, P., Verma, P., Kandikonda, M., Lakhani, A., 2019. Pollution characteristics, human health risk through multiple exposure pathways, and source apportionment of heavy metals in PM_{10} at Indo-Gangetic site. Urban Clim. 27, 149-162.

Sánchez-Rodas, D., Alsioufi, L., Sánchez de la Campa, A.M., González-Castanedo, Y., 2017. Antimony speciation as geochemical tracer for anthropogenic emissions of atmospheric particulate matter. J. Hazard. Mater. 324, 213-220.

SDA - Secretaría Distrital de Ambiente, 2018. Informe anual de calidad del aire de Bogotá, 2017. Bogotá, SDA/Alcaldía Mayor de Bogotá.

SDA, 2017. Informe anual de calidad del aire de Bogotá, 2016. Bogotá, SDA/Alcaldía Mayor de Bogotá.

SDA, 2010. Guía para la gestión y manejo integral de residuos. Industria metalmecánica. Bogotá, SDA/Universidad Distrital Francisco José de Caldas.

SDA, 2009. Elementos técnicos del Plan Decenal de Descontaminación de Bogotá. Parte 1: Caracterización de material particulado y modelos receptores. Bogotá, Alcaldía Mayor de Bogotá/Universidad de los Andes.

SDM - Secretaría Distrital de Movilidad, 2017. Observatorio Ambiental de Bogotá. Indicadores de movilidad sostenible. Bogotá, Secretaría Distrital de Ambiente. Data obtained from http://oab.ambienteBogota.gov.co/es/temas?v=6&p=21 (accessed 08 May 2019).

Sun, Y., Hu, X., Wu, J., Lian, H., Chen, Y., 2014. Fractionation and health risks of atmospheric particle-bound As and heavy metals in summer and winter. Sci. Total Environ. 493, 487-494.

Susaya, J., Kim, K., Ahn, J., Jung, M., Kang, Ch., 2010. BBQ charcoal combustion as an important source of trace metal exposure to humans. J. Hazard. Mater. 176, 932-937.

Suvarapu, L., Baek, S., 2017. Determination of heavy metals in the ambient atmosphere: a review. Toxicol. Ind. Health 33(1), 79-96.

Tan, J., Duan, J., Ma, Y., Yang, F., Cheng, Y., He, K., Yu, Y., Wang, J., 2014. Source of atmospheric heavy metals in winter in Foshan, China. Sci. Total Environ. 493, 262-270.

The World Bank, 2016. Life expectancy at birth, total (years). Data obtained from https://data.worldbank.org/indicator/SP.DYN.LE00.IN?locations=CO (accessed 18 April 2019).

Thorpe, A., Harrison, R., 2008. Sources and properties of non-exhaust particulate matter from road traffic: a review. Sci. Total Environ. 400, 270-282.

UN - United Nations, 2008. International Standard Industrial Classification of All Economic Activities, Revision 4. New York, Department of Economic and Social Affairs.

UNEP - United Nations Environment Programme, 2016. Global Environment Outlook (GEO-6). Regional Assessment for Latin America and the Caribbean. Nairobi, United Nations Environment Programme.

US EPA, 2014. EPA Positive Matrix Factorization (PMF) 5.0. Fundamentals & User Guide. NC, Research Triangle Park.

US EPA, 2011. Exposure Factors Handbook: 2011 Edition. Washigton D.C., U.S. Environmental Protection Agency.

US EPA, 2009. Risk Assessment Guidance for Superfund Volume I: Human Health Evaluation Manual (Part F, Supplemental Guidance for Inhalation Risk Assessment). Washington D.C., US Environmental Protection Agency.

US EPA, 2001. Baseline human health risk assessment. Vasquez Boulevard and I-70 Superfund site Denver, CO. Denver, US Environmental Protection Agency.

Valdés, A., Polvé, M., Munoz, M., Toutain, J., Morata, D., 2013. Geochemical features of aerosols in Santiago de Chile from time series analysis. Environ. Earth Sci. 69, 2073-2090.

Vargas, F., Rojas, N., Pachón, J., Russell, A., 2012. PM_{10} characterization and source apportionment at two residential areas in Bogota. Atmos. Pollut. Res. 3, 72-80.

Wang, X., He, Sh., Chen, Sh., Zhang, Y., Wang, A., Luo, J., Ye, X., Mo, Z., Wu, L., Xu, P., Cai, G., Chen, Z., Lou, X., 2018a. Spatiotemporal characteristics and health risk assessment of heavy metals in $PM_{2.5}$ in Zhejiang province. Int. J. Environ. Res. Public Health 15, 583.

Wang, X., Wang, Y., Bai, Y., Wang, P., Zhao, Y., 2018b. An overview of physical and chemical features of diesel exhaust particles. J. Energy Inst. (in press).

WHO - World Health Organization, 2016. World Health Statistics 2016. Geneva, World Health Organization.

WHO, 2008. Health risks of heavy metals from long-range transboundary air pollution. Copenhagen, WHO Regional Office for Europe.

Wu, D., Sun, Sh., 2016. Speciation analysis of As, Sb and Se. Trends Environ. Anal. Chem. 11, 9-22.

Zannoni, D., Valotto, G., Visin, F., Rampazzo, G., 2016. Sources and distribution of tracer elements in road dust: the Venice mainland case of study. J. Geochem. Explor. 166, 64-72.

Zhang, Y., Cai, J., Wang, Sh., He, K., Zheng, M., 2017. Review of receptor-based source apportionment research of fine particulate matter and its challenges in China. Sci. Total Environ. 586, 917-929.

Zhao, L., Hu, G., Yan, Y., Yu, R., Cui, J., Wang, X., Yan, Y., 2019. Source apportionment of heavy metals in urban road dust in a continental city of eastern China: using Pb and Sr isotopes combined with multivariate statistical analysis. Atmos. Environ. 201, 201-211.

Zheng, J., Ohata, M., Furuta, N., 2000. Studies on the speciation of inorganic and organic antimony compounds in airborne particulate matter by HPLC-ICP-MS. Analyst 125, 1025-1028.

Zhou, J., Tian, H., Zhu, Ch., Hao, J., Gao, J., Wang, Y., Xue, Y., Hua, Sh., Wang, K., 2015. Future trends of global atmospheric antimony emissions from anthropogenic activities until 2050. Atmos. Environ. 120, 385-392.

Zhou, S., Yuan, Q., Li, W., Lu, Y., Zhang, Y., Wang, W., 2014. Trace metals in atmospheric fine particles in one industrial urban city: spatial variations, sources, and health implications. J. Environ. Sci. 26, 205-213.

Zhu, T., Melamed, M., Parrish, D., Gauss, M., Gallardo, L., Lawrence, M., Konare, A., Liousse, C., 2012. Impacts of megacities on air pollution and climate. Geneva, WMO/IGAC.

Zoller, W., Gladney, E., Duce, R., 1974. Atmospheric concentrations and sources of trace metals at the South Pole. Science 183, 199-201.